

AD-A229 914

7 Nov 89

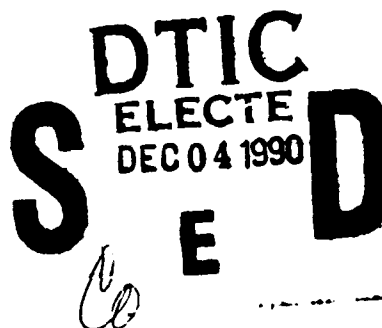
Conference Presentation

Unsteady Pressure Loads from Plunging Airfoils TA 2307-F1-38

E. Stephen, C. Kedzie, M. Robinson

F.J. Seiler Research Laboratory  
USAF Academy CO 80840-6528

FJSRL-PR-90-0019



Distribution Unlimited

Forced unsteady flow separation from a dynamically plunging airfoil was investigated using surface mounted pressure transducers. The transient pressure distributions and integrated lift and drag coefficients were plotted for parametric alterations in mean angle of attack, reduced amplitude and reduced frequency. The unsteady loads produced were strongly dependent upon the dynamic stall event. Dynamic similarity for dimensional scaling of plunging motions was shown to be a function of both reduced frequency and amplitude.

dynamic loads  
flow separation  
unsteady flow

9

UNCLASSIFIED

UNCLASSIFIED

UNCLASSIFIED

NONE

# Unsteady Pressure Loads from Plunging Airfoils

Eric Stephen\*  
Frank J. Seiler Research Laboratory  
USAF Academy

Chris Kedzie\*\*  
Department of Aeronautics  
USAF Academy

Michael C. Robinson\*\*\*  
Department of Aeronautics  
USAF Academy



DTIC GRA&I	
DTIC TAB	
Unannounced	
Justification	
By	
Distribution/	
Availability Codes	
Dist	Avail and/or Special
A-1	

## Abstract

Forced unsteady flow separation from a dynamically plunging airfoil was investigated using surface mounted pressure transducers. The transient pressure distributions and integrated lift and drag coefficients were plotted for parametric alterations in mean angle of attack, reduced amplitude and reduced frequency. The unsteady loads produced were strongly dependent upon the dynamic stall event. Dynamic similarity for dimensional scaling of plunging motions was shown to be a function of both reduced frequency and amplitude

These experiments focused on the unsteady separation produced by an airfoil driven sinusoidally in pure plunge. The reduced frequency, reduced amplitude and mean angle of attack were examined parametrically. Unlike the pitching airfoil motion, dynamic similarity for sinusoidal plunge can be achieved using  $k$ ,  $\lambda$ , and  $\alpha_0$ . The effects of these parameters on the separated flow and the interdependence on dimensional scaling are discussed.

## Nomenclature

- $c$  chord length
- $C_d$  coefficient lift
- $C_l$  coefficient drag
- $C_p$  coefficient pressure
- $f$  oscillation frequency
- $h$  oscillation amplitude
- $k$  reduced frequency ( $\omega c/2V_\infty$ )
- $t$  time
- $V_\infty$  free stream velocity
- $\alpha$  incidence angle  $\alpha_0 + \alpha_i$
- $\alpha_0$  mean angle of attack
- $\alpha_i$  induced angle of attack  $-\tan^{-1}[\lambda \cos(\omega t)]$
- $\lambda$  reduced amplitude ( $h\omega/V_\infty$ )
- $\omega$  oscillation rate ( $2\pi f$ )

## Introduction

Forced unsteady separated flow from plunging airfoils has many of the same dynamic characteristics as pitching airfoils.<sup>1,2</sup> When the airfoil is driven through the static stall angle, dynamic stall ensues.<sup>1</sup> Attempts to match the relative motions between pitching and plunging airfoils using equivalent angles<sup>1,3</sup> has failed to produce dynamic similarity. Recent observations by Ericsson and Reding<sup>4</sup> suggest that the "leading edge jet" effect may explain some of the differences between the two motions.

\* Chief, Aeromechanics, member AIAA  
\*\* Research Associate, member AIAA  
\*\*\* Visiting Professor, Dept. of Aerospace Engineering, Univ. of Colorado, member AIAA

## PRESSURE PORT

## LOCATION

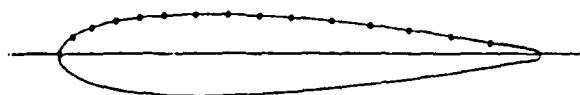


Figure 1. Positions of the pressure ports for the transducers close coupled with the surface

## Apparatus and procedure

The tests were performed in the Frank J. Seiler low speed wind tunnel located at the United States Air Force Academy. The tunnel has a 3' by 3' test section and a wind speed capability from 10 to 100 fps.

A 6" chord NACA 0015 aluminum airfoil instrumented with 15 miniature Endevco pressure transducers was used for these experiments. The pressure transducer locations are shown in fig. 1. Splitter plates attached to the airfoil provided two dimensional flow. Data from the pressure transducers were collected using a Masscomp data acquisition system. Two hundred points were collected for each oscillation cycle. Forty five successive cycles were averaged together for a complete data run.

The sinusoidal plunge drive mechanism is shown in fig. 2. The airfoil with the two splitter plates was attached to the 19" by 22" base of the drive mechanism. The figure shows the top view of the fixture with the base removed. The mounting base plate was attached to the sliding bearings indicated by the shaded regions of fig. 2. Sinusoidal motion of the base plate was produced by rotating the center fitting with a programmable stepper motor. An adjustable arm was slid in and out of the fitting to adjust the amplitude of the plunging motions.

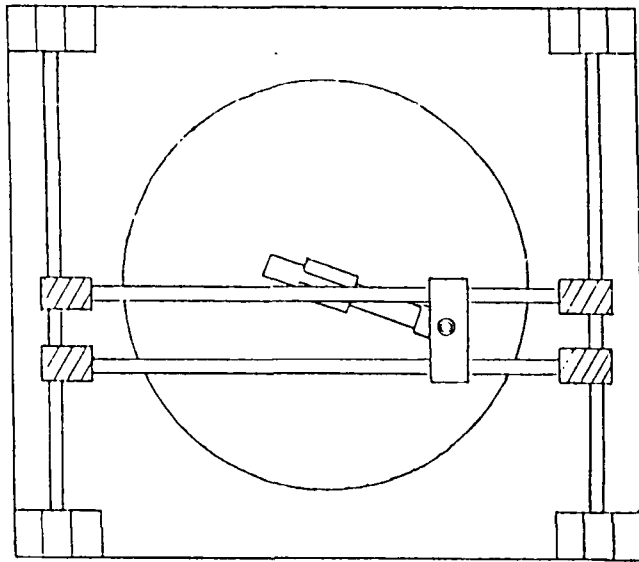


Figure 2. Plunge Oscillating Mechanism, mounting plate attached at the cross-hatched areas

The test matrix, shown in Tables 1-3, was designed to examine the parametric effects of mean angle, reduced amplitude and reduced frequency. Unfortunately, the d.c. stepper motor rotation rate was extremely limited (6 Hz). In order to examine high reduced frequencies, the tunnel velocity was lowered to 15 fps. Increased noise at these levels made the pressure magnitude results suspect. Future investigations will be required to confirm these magnitudes using a different drive apparatus.

Table 1. Mean angle of attack changes

k	$\alpha_1^\circ$	f(Hz)	V (fps)	h(in)	$\alpha_0^\circ$
0.1	10	2.55	40	5.29	0
"	"	"	"	"	5
"	"	"	"	"	10
"	"	"	"	"	15
"	"	"	"	"	20
"	"	"	"	"	25

Table 2. Frequency changes

k	$\alpha_1^\circ$	f(Hz)	V (fps)	h(in)	$\alpha_0^\circ$
0.1	10	2.55	40	5.29	15
0.2	"	3.82	30	2.65	"
0.3	"	3.82	20	1.76	"
0.4	"	5.09	20	1.32	"
0.5	"	4.77	15	1.06	"

Table 3. Reduced amplitude changes

k	$\alpha_1^\circ$	f(Hz)	V (fps)	h(in)	$\alpha_0^\circ$
0.1	10	2.55	40	5.29	15
"	8	"	"	4.21	"
"	6	"	"	3.15	"
"	4	"	"	2.09	"
"	2	"	"	1.05	"

## Results

Forced unsteady separation from a plunging airfoil has many of the same attributes observed with pitching airfoils. Previous investigations<sup>1,3</sup> have noted the formation of a dynamic stall vortex when a plunging airfoil exceeds the induced static stall angle of attack. These results demonstrate the sensitivity of dynamic stall to the plunging motion history and airfoil geometry.

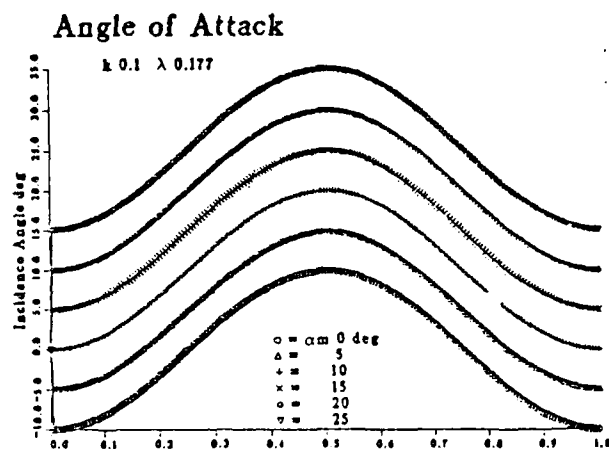
In order to achieve dynamic similarity in sinusoidal plunging airfoil motion, it is necessary to match both the reduced frequency (k) and the reduced amplitude ( $\lambda$ ). Although both parameters are dependent on the oscillation rate ( $\omega$ ), they alter the flow field characteristics in dissimilar ways. Parametric changes in the mean angle of attack ( $\alpha_0$ ), reduced amplitude ( $\lambda$ ) and reduced frequency (k) cause significant alterations in dynamic stall development and the resulting transient loads incurred.

## Mean angle of attack

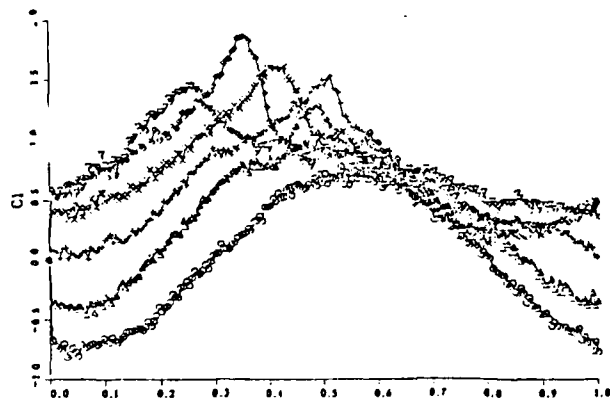
Increasing the mean angle of attack of a plunging airfoil produced the same general effect observed with airfoils driven with pitching motion histories: (1) it was necessary to exceed the static stall angle in order to produce dynamic separation, (2) increasing  $\alpha_0$  initiated vortex development earlier in the oscillation cycle.

At mean angles of  $0^\circ$  and  $5^\circ$  (fig. 3), flow remained attached throughout the oscillation cycle. The maximum induced incidence angle did not exceed the value required to initiate dynamic stall.

## Mean Angle Effects



### Lift Coefficient



### Drag Coefficient

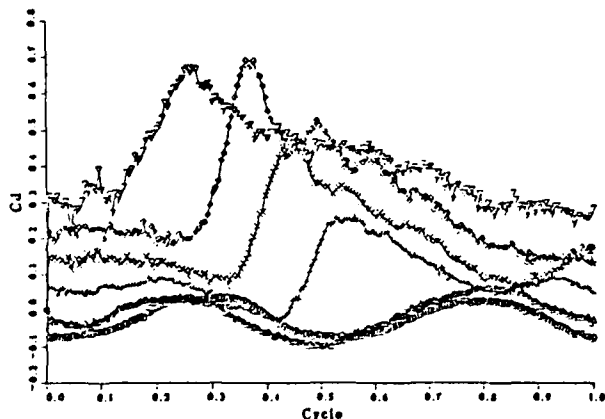


Figure 3. Mean Angle Effects on Unsteady Force Profiles

## Mean Angle Effects

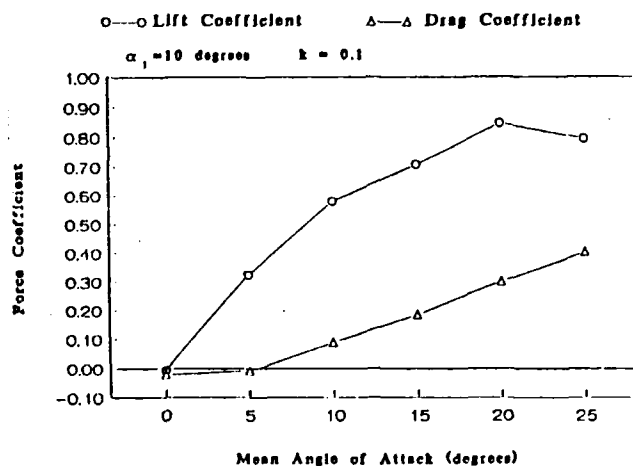


Figure 4. Mean Angle Effect on Time Averaged Forces

At these low mean angles, thrust was produced during both the up and down stroke portions of the oscillation cycle. Cycle averaged lift and drag values (fig. 4) indicate a net positive pressure thrust. Propulsive wake signatures from rapidly plunging airfoils have previously been observed by Freymuth<sup>5</sup> at larger reduced amplitudes ( $\lambda > 0.23$ ). The double thrust behavior can be explained by the change in the direction of the lift vector through the oscillation cycle. With rapid oscillations, the induced angle orients the lift vector upstream producing a thrust component.<sup>5</sup> Larger reduced amplitudes should produce even greater net thrust values.

The first indication of vortex initiation occurred at a mean angle of  $10^\circ$ .  $C_l$  peaked with the vortex formation at approximately 0.5 cycle ( $\alpha_i = 20^\circ$ ). Correspondingly,  $C_d$  also rapidly increased. Further increases in mean angle promoted vortex initiation earlier in the oscillation cycle with larger  $C_l$  and  $C_d$  values.

A clear indication of vortex development can also be observed in the upper surface pressure data shown in fig. 5. The characteristic pressure signature of a vortex converging over the airfoil chord occurs in the 10, 15 and  $20^\circ$   $\alpha_0$  profiles. At  $25^\circ$  vortex development is not as clear, however, there is evidence of dynamic attachment. The pressure rise followed by a small but definitive pressure track are indicative of disparate vortical development.

### Reduced amplitude

The reduced amplitude and induced angle of attack effects are equivalent ( $\alpha_i = \tan^{-1}[\lambda]$ ). The induced angle of

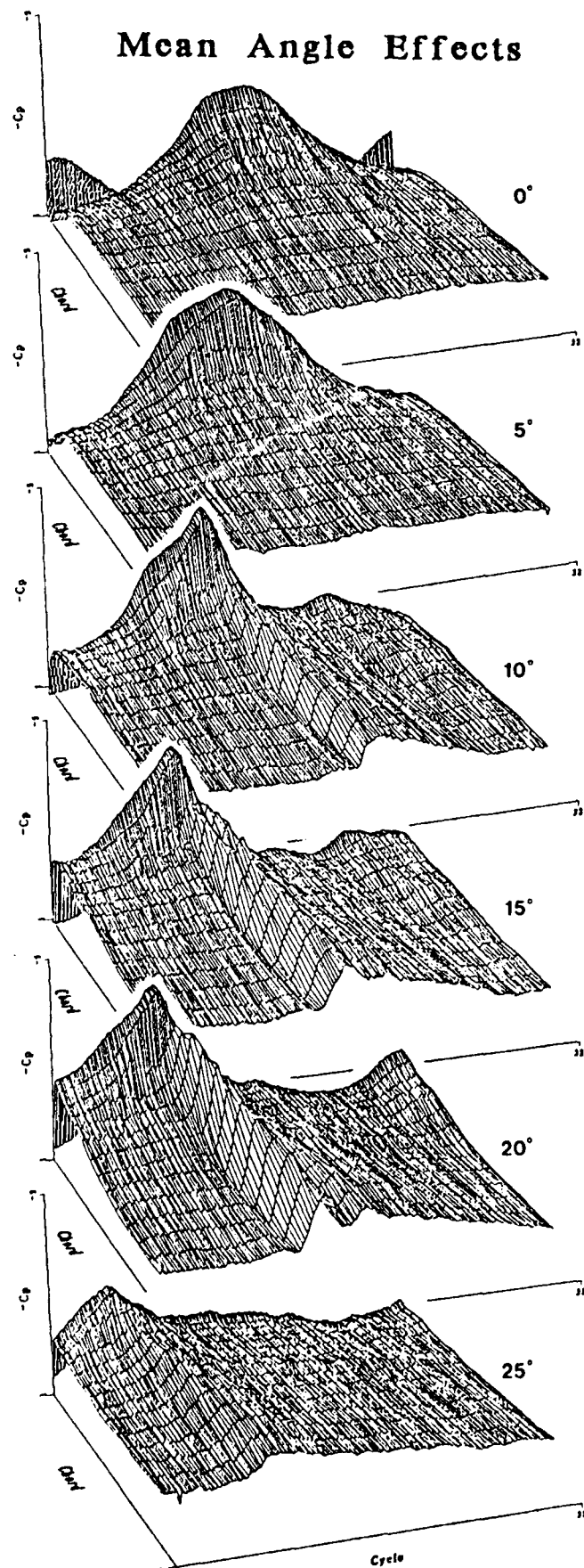


Figure 5. Mean Angle Effects on Pressure Profiles  $\alpha_0 = 0, 5, 10, 15, 20, 25$

attack in plunging motions is comparable to the oscillation angle with pitching airfoil motions. There are, however, notable differences in the boundary conditions between the two motions which will be discussed later.

In general, alterations in vortex initiation and development with  $\alpha_i$  did not parallel oscillation angle changes with pure pitching motions. Increased  $\alpha_i$  initiated vortex development earlier in the oscillation cycle and no appreciable increase in  $C_l$  was observed after dynamic stall was achieved.

Dynamic stall was not achieved until the static stall limitation was exceeded (approximately  $12^\circ$  for the low Reynolds numbers tested here). An induced angle of attack of  $2^\circ$  (fig. 6) did not sufficiently penetrate the lower static stall angle to attach the separated flow.

For  $\alpha_i$  values  $\geq 4^\circ$ , dynamic stall was achieved. The peak lift coefficient continued to increase until an induced angle of  $6^\circ$  was reached. Further increases in  $\alpha_i$  increased only  $C_d$ . Also, increases in  $\alpha_i$  initiated vortex development earlier in the oscillation cycle.

Upper surface pressure data (fig. 7) show the distinctive vortex convection for  $\alpha_i > 2^\circ$ . Unlike the pressure data from oscillating airfoils, the peak pressures obtained over the leading edge remain fairly constant with increasing  $\alpha_i$ . The temporal gradient pressure change is much larger with higher  $\alpha_i$ . Integration of  $C_l$  and  $C_d$  (fig. 8) over the plunging cycle showed little net benefit from vortex development with increasing  $\alpha_i$ .

#### Reduced frequency

The physical limitation of the stepper motor drive severely limited the reduced frequency range. Although  $k$  values of 0.1 were all collected at tunnel velocities of 40 fps, it was necessary to reduce the free stream velocities to 30, 20, 20 and 15 fps in order to achieve  $k$  values of 0.2, 0.3, 0.4, and 0.5 respectively. Although Reynolds number effects would probably not affect the results, the inherently small signal to noise ratio at velocities below 20 fps could be a problem. Hence, these higher  $k$  values are presented to show the temporal trends in vortex development as a function of the oscillation cycle. Verification of the actual  $C_l$  and  $C_d$  magnitudes will be performed at a later date with a different drive apparatus and at higher tunnel speeds.

Increasing the reduced frequency while maintaining a constant  $\lambda$  ( $\alpha_i$ ) produced results similar to those obtained with airfoils oscillating in pitch. Vortex initiation is delayed with increasing plunge rate for an appreciable

## Reduced Amplitude Effects

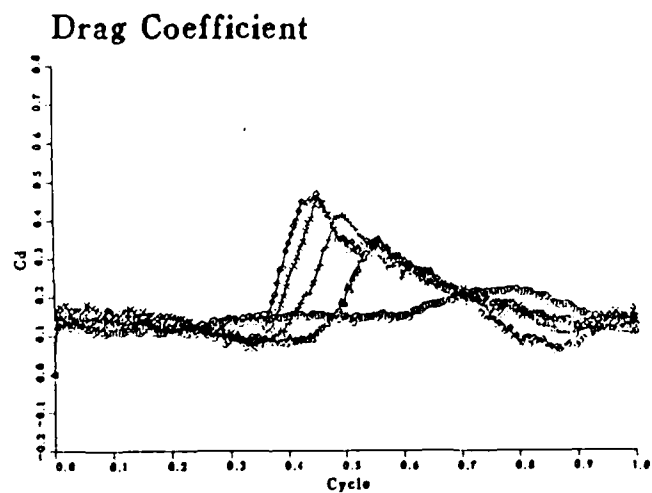
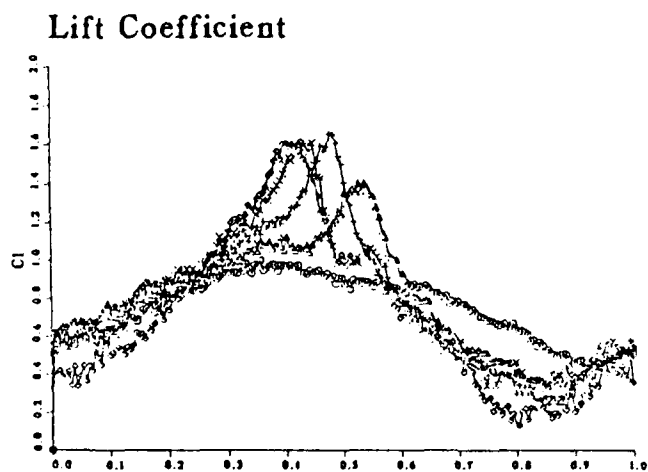
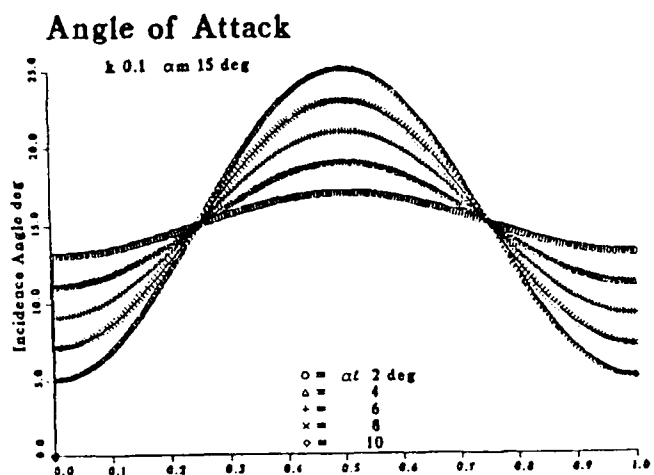


Figure 6. Reduced Amplitude Effects on Unsteady Force Profiles

## Reduced Amplitude Effects

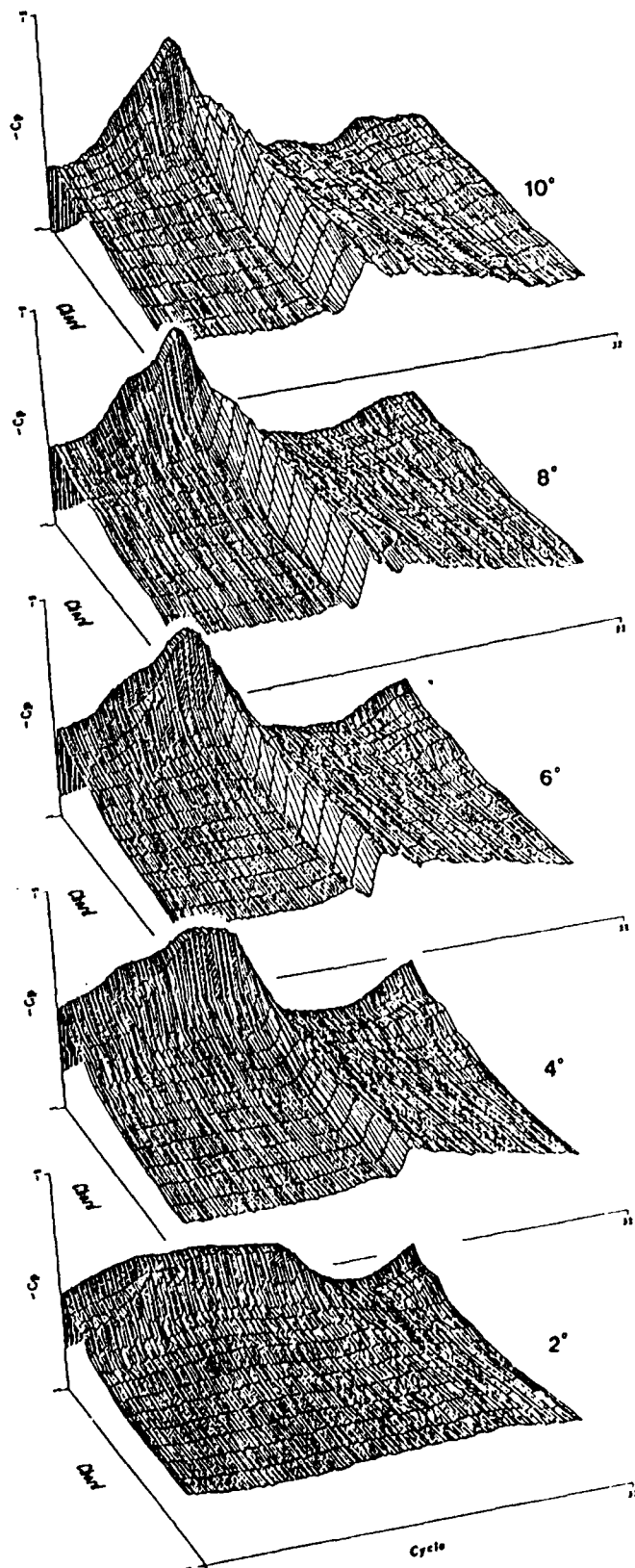


Figure 7. Reduced Amplitude Effects on Pressure Profiles  $\alpha_1 = 10, 8, 6, 4, 2$

## Reduced Amplitude Effects

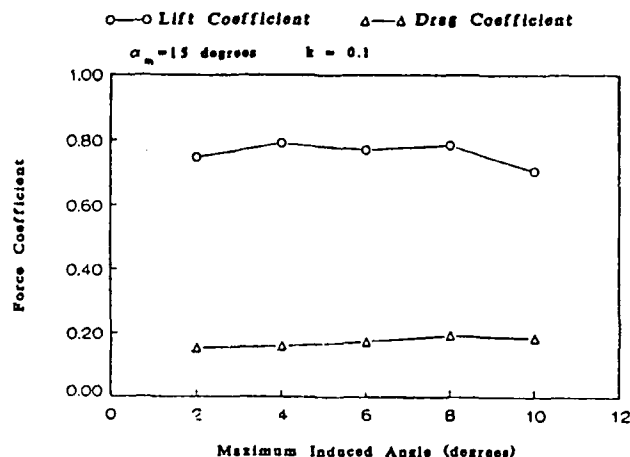


Figure 8. Reduced Amplitude Effects on Time Averaged Forces

portion of the oscillation cycle (fig. 9). Although the peak  $C_l$  increases from  $k=0.1$  to 0.2, this increase in peak magnitude did not continue with higher  $k$  values. Again, it is not clear whether this result is genuine or a function of increased experimental error at low velocities.

The most notable effect of reduced frequency is the increased residence time of the dynamic stall vortex. The lift and drag data (fig. 9) as well as the upper surface pressure profiles show the increased residence as a function of the plunging cycle. Cycle averaged integrations of  $C_l$  and  $C_d$  (fig. 10) also suggest a lift enhancement with increasing  $k$  without a corresponding drag penalty. However, the same disclaimer on averaged load magnitudes must apply.

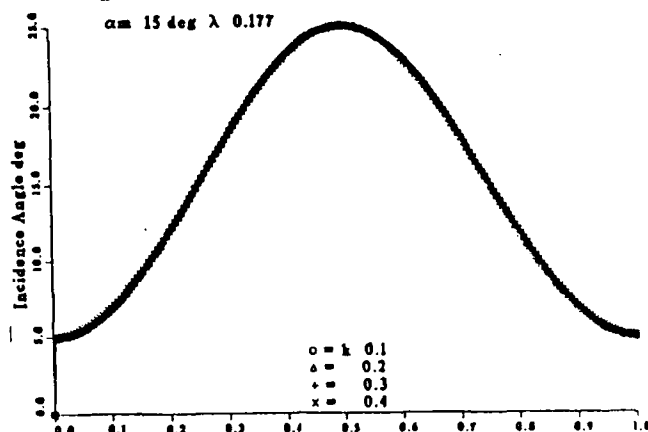
### Discussion

Forced unsteady separation from an airfoil driven with sinusoidal plunging motions is very similar to dynamic stall events initiated from airfoils oscillating in pitch. However, as demonstrated by Carta and Maresca et. al.,<sup>3</sup> and discussed by Ericsson and Reding,<sup>4</sup> significant variations in experimental results occur when dynamic scaling between these motions is attempted using an equivalent angle approach. Due to differences in the total surface boundary conditions (surface motions) between rotational and translational motion histories, an exact dynamic similarity parameter cannot be achieved.

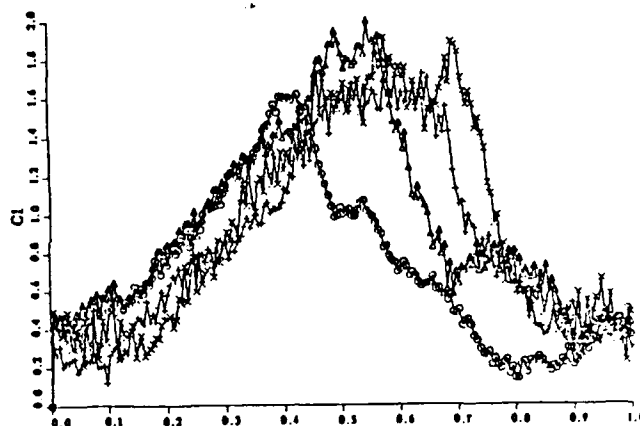
Dynamic similarity for plunging airfoil motions is a two parameter problem. The reduced amplitude and reduced frequency must both be matched simultaneously in order to achieve equivalent spatial and temporal boundary

## Reduced Frequency Effects

### Angle of Attack



### Lift Coefficient



### Drag Coefficient

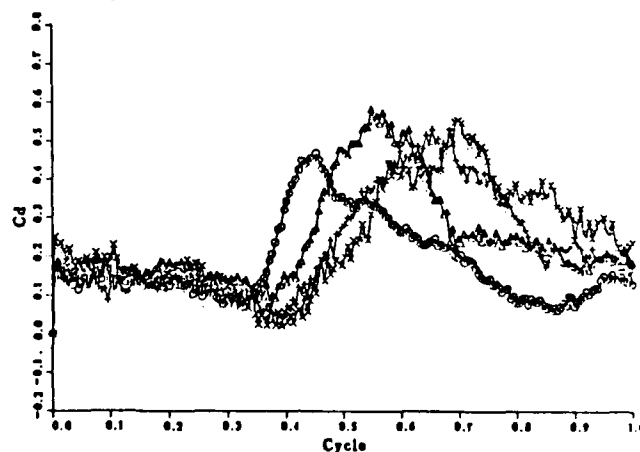


Figure 9. Reduced Frequency Effects on Unsteady Force Profiles

## Reduced Frequency Effects

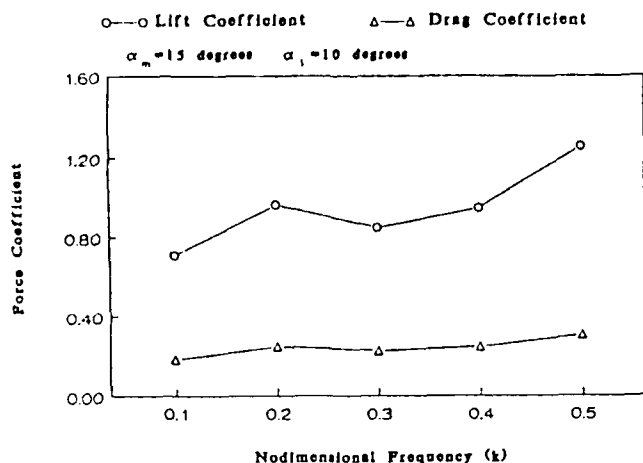


Figure 10. Reduced Frequency Effects on Time Averaged Forces

conditions. The reduced amplitude scales the induced angle of attack and provides for the proper "quasi-steady" geometric condition. The reduced amplitude also dictates the magnitude of the "leading edge jet effect" postulated by Ericsson and Reding.<sup>4</sup>

Parametric changes in the induced angle of attack clearly show the influence of the reduced amplitude parameter. Increasing the incidence angle initiated vortex development earlier in the plunging cycle. This effect is contrary to the results obtained with increased oscillation angles for pitching motions. Vortex initiation is delayed for the same "equivalent" angle conditions.

Earlier vortex initiation for plunging airfoils can be explained in terms of the leading edge jet effect. Increasing the oscillation angle (pitching) or incidence angle (plunging) for a set reduced frequency forces the airfoil to move more rapidly. The increased surface motion also increases the leading edge jet effect. The leading edge jet influence is of opposite sign for the two motions, delaying stall for the pitching motion and promoting stall for the plunging motion.<sup>4</sup>

In contrast, the reduced frequency parameter scales the fluid response times to the oscillation cycle. Slow reduced frequencies yield quasi-steady results. The dominate force effects at low  $k$  values are provided by the reduced amplitude (incidence angle). Large reduce frequencies directly affect vortex initiation and development in cyclic motions. This effect is due to the viscous time scales which govern vorticity diffusion, accumulation, separation and convection. Also, rapid oscillations permit vortex residence over the airfoil chord for large portions of the

oscillation cycle which bias the transient loading.

The influence of reduced frequency on vortex development for plunging airfoils was similar to that of pitching airfoils. Increasing the reduced frequency delayed vortex initiation and increased vortex residence time.

At first glance, this result may seem contrary to the leading edge jet effect discussed above. It is, however, consistent when the relative effects of reduced frequency and reduced amplitude are separated. For plunging motions, the reduced frequency can be increased without changing the relative airfoil motion by simultaneously decreasing the pitching amplitude. In this manner, both the magnitude of the incidence angle and

## Reduced Frequency Effects

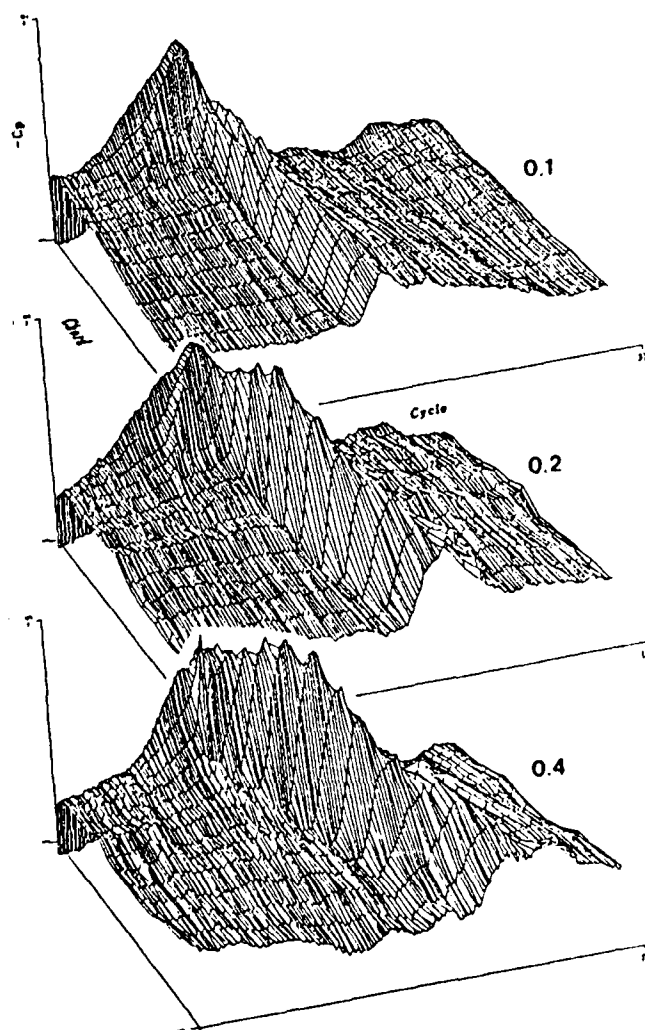


Figure 11. Reduced Frequency Effect on Pressure Profiles  $k=0.1, 0.2, 0.4$



leading edge jet effect can remain constant

For pitching motions, there is no equivalent variable manipulation. Increasing  $k$  while simultaneously decreasing the oscillation angle will hold the relative airfoil motion constant but the incidence angle will decrease. Increasing  $k$  without changing the oscillation angle holds the incidence angle constant but increases the airfoil motion and the leading edge jet effect.

For plunging motions, delays in vortex initiation with increasing  $k$  appear to be a function of temporal scaling. The initiation of the dynamic stall vortex is dependent upon the viscous time scales governing diffusion and accumulation of vorticity. Given the matched induced angle profiles, the delay in vortex development is probably due to the skewed time base at high  $k$  values. Vortex development plotted as a function of non-dimensional time would be a better representation of the initiation and convection history and would remove any motion history bias.

#### Conclusions

Forced unsteady separation induced from a plunging airfoil can produce the same dynamic stall characteristics observed with pitching airfoils. The reduced frequency and amplitude parameters affect the separation process in different ways. Reduced amplitude governs the leading edge jet effect and initiates stall earlier in the oscillation cycle. Reduced frequency scales the vorticity production to the cycle motion. Larger  $k$  values appear to delay stall as a function of the oscillation cycle. Both reduced frequency and amplitude must be matched in order to achieve dynamic similarity for plunging motions. Further investigations are required to validate the attenuation of peak transient loads observed at higher  $k$  values.

#### Acknowledgements

This work has been sponsored by the Air Force Office of Scientific Research WU 2307f1-38.

#### References

- <sup>1</sup>Carta, F.O., "A Comparison of the Pitching and Plunging Response of an Oscillating Airfoil," NASA CR 3172, Oct. 1979.
- <sup>2</sup>Carr, L.W., McAlister, K.W., and McCroskey, W.J., "Analysis of Development of Dynamic Stall Based on Oscillating Airfoil Experiments," NASA TN D8382, 1977.
- <sup>3</sup>Maresca, C.A., Favier, D.J., and Rebont, J.M., "Unsteady Aerodynamics of an Aerofoil at High Angle of Incidence Performing Various Linear Oscillations in a Uniform Stream," Journal of the American Helicopter Society, Vol. 13, Apr. 1981, pp. 40-45.
- <sup>4</sup>Ericsson, L.E. and Reding, J.P., "Unsteady Flow Concepts for Dynamic Stall Analysis," Journal of Aircraft, Vol. 2, No. 8, pp. 601-606.
- <sup>5</sup>Freythuth, P., "Propulsive Vortical Signatures of Plunging and Pitching Airfoils," AIAA Journal, Vol. 26, No. 7, July 1988, pp. 881-883. Presented earlier as AIAA paper 88-0323, Jan. 1988, pp. 1-11.